Cholesteric elastomers: Deformable photonic solids

Y. Mao, E. M. Terentjev, and M. Warner
Cavendish Laboratory, University of Cambridge, Madingley Road, Cambridge, CB3 0HE, United Kingdom
(Received 24 May 2001; published 24 September 2001)

A mechanical strain applied to a monodomain cholesteric elastomer modulates and eventually unwinds the helical director distribution. There are similarities with the classical problem of an electric field applied to a cholesteric liquid crystal, but also differences. Frank elasticity is of minor importance unless the gel is very weak. The interplay is rather between the director being helically anchored to the rubber elastic matrix and the external mechanical field. Stretching perpendicular to the helix axis induces the uniform unwound state via the elimination of sharp, pinned twist walls above a critical strain. Below the critical strain the coarsening of the director distribution is not accompanied by an increase but rather by an affine decrease in the pitch. Unwinding through conical director states occurs when the elastomer is stretched along the helical axis. Finally we consider cholesteric elastomers in a classical device geometry with an electric field applied along the pitch axis and hence transverse to the director orientation.

DOI: 10.1103/PhysRevE.64.041803 PACS number(s): 61.30.−v, 61.41.+e, 78.20.Ek

I. INTRODUCTION

Monodomain cholesteric elastomers are formed by crosslinking mesogenic chiral polymers in the cholesteric state with a properly formed helical director twist. The subsequent retention of the helical state as an elastic equilibrium [1] is a natural topological consequence of textures contained within the crosslinked network, seen in a number of other elastomers with liquid crystalline order and other microstructure. Symmetrical biaxial extension, applied to a sample film in the process of crosslinking, aligns the director uniformly in the film plane, and thus the cholesteric helix axis along the sample normal [2]. The more subtle imprinting route [3] to achieving chiral elastomers without material of intrinsic chirality have been demonstrated [4] and theoretically described [5].

Such elastomers combine all the optical properties of twisted nematic liquids with the remarkable mechanical characteristics of rubbers, and there are important device applications such as color displays [6,7], a chiral pump for sorting racemic solvents [8], memory storage [9] and even lasing [10,11]. Thanks to the one dimensional (1D) photonic gap arising from its helical structure, an elastomer laser requires no mirrors to create a cavity and has a very low lasing threshold. Furthermore, it exhibits strong optomechanical coupling, with the laser color depending sensitively on the strain applied. Such a mechanically tunable laser could hugely benefit optical fiber communication. It is therefore important to consider the mechanical possibilities of such solids with a helical microstructure. We expect new transitions and instabilities characteristic of liquid crystalline elastomers [12]. There is some experimental evidence [2,13] that such effects are indeed observable and our hope is that this theoretical work will stimulate more studies in this field.

II. MECHANICAL DEFORMATION

Consider a monodomain cholesteric elastomer with an ideal helically twisted director $\mathbf{n}_0(z)$ in the x-y plane, initially making angle $\phi_0 = q_0 z$ with the x axis, Fig. 1. We shall examine two specific cases of imposed uniaxial extension: (i) transverse deformation $\lambda_{xx} = \lambda$, in the plane including $\mathbf{n}_0$, and (ii) longitudinal deformation along the helix axis $\lambda_{zz} = \lambda$.

The symmetry obvious from Fig. 1 requires that in the case (i) the director remains in the x-y plane, characterized by the azimuthal angle $\phi(z)$, while in the case (ii) one may expect a conical texture with $\mathbf{n}(z)$ inclined towards the stretching axis z and therefore described by two angles θ and ϕ (cf. Fig. 4). In ordinary liquid cholesterics subjected to, e.g., a magnetic field H_z, such conical states are not generally seen, preempted by the 90° switching of the helix axis and then untwisting in the ''transverse'' geometry [14,15]. We shall see that in elastomers, due to the director anchoring, this regime is not possible and the conical director configurations should occur.

An elastic material with a microstructure represented by an independently mobile director orientation is analogous to Cosserat media. In the limit of linear elasticity the relative rotation coupling between the director rotation $\boldsymbol{\omega} = [\mathbf{n} \times \delta\mathbf{n}]$ and the antisymmetric part of strain, $\Omega_i = \epsilon_{ijk}\varepsilon_{jk}$ (with summation convention),

$$\tfrac{1}{2}D_1[\mathbf{n}\times(\boldsymbol{\Omega}-\boldsymbol{\omega})]^2 + D_2\mathbf{n}\cdot\underline{\underline{\varepsilon}}^{(s)}\cdot[\mathbf{n}\times(\boldsymbol{\Omega}-\boldsymbol{\omega})], \qquad (1)$$

has been first written down phenomenologically by de Gennes [16], $\underline{\underline{\varepsilon}}^{(s)}$ being the symmetric part of the small strain defined as $\underline{\underline{\varepsilon}} = \underline{\underline{\lambda}} - \underline{\underline{\delta}}$. The deformation tensor $\underline{\underline{\lambda}}$ is related to the displacement vector $\underline{u}(\underline{r})$ via

$$\lambda_{ij} = \nabla_j u_i ,$$

where subscripts i and j refer to x, y, and z. The symmetry-based expression (1) is only valid for small deformations, having only linear and quadratic terms in the local relative rotation.

The microscopic statistical-mechanical theory of nematic rubber elasticity, summarized in Ref. [17], obtains a frame-independent generalization of the classical rubber-elastic energy density,

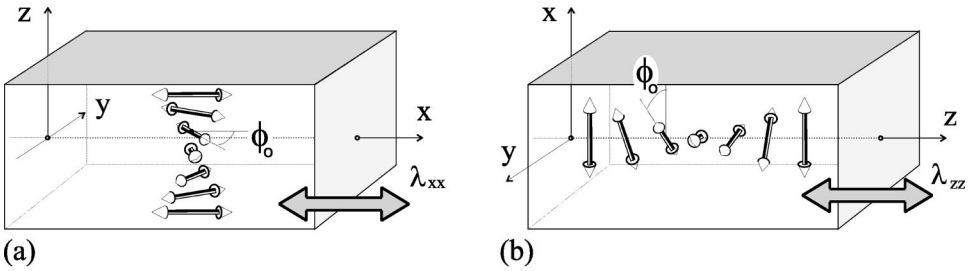

FIG. 1. The initial director $\mathbf{n}_0(z)$ in a cholesteric helix makes an azimuthal angle $\phi_0 = q_0 z$ with the x axis; the helical pitch is $p = \pi/q_0$. Two principal directions of mechanical deformation, (a) λ_{xx} and (b) λ_{zz}, are shown by arrows.

$$F = \tfrac{1}{2}\mu \,\mathrm{Tr}(\underline{\underline{\ell}}_0 \cdot \underline{\underline{\lambda}}^T \cdot \underline{\underline{\ell}}^{-1} \cdot \underline{\underline{\lambda}}), \tag{2}$$

plus the constraint of material incompressibility, expressed by the condition $\det(\lambda) = 1$, on the strain tensor. Apart from the strain, the other entries in Eq. (2) are

$$\underline{\underline{\ell}}_0 = l_\perp \underline{\underline{\delta}} + (\ell_\parallel - \ell_\perp)\mathbf{n}_0\mathbf{n}_0,$$
$$\underline{\underline{\ell}}^{-1} = (1/\ell_\perp)\underline{\underline{\delta}} + (1/\ell_\parallel - 1/\ell_\perp)\mathbf{n}\mathbf{n}, \tag{3}$$

the reduced shape and inverse shape tensors characterizing the Gaussian distribution of nematic polymer chains before and after the distortion $\underline{\underline{\lambda}}$. The rubber shear modulus $\mu = n_s k_B T$ (with n_s the number density of network strands, proportional to the crosslink density) is that characteristic of the underlying isotropic rubber and sets the energy scale of distortions. The free-energy density (2) is known to be valid up to large strains and correctly predicts the optomechanical responses and the soft elasticity of nematic elastomers. The free-energy F is a function only of the chain anisotropy $r = \ell_\parallel/\ell_\perp$, the ratio of the effective step lengths parallel and perpendicular to the director. It is an independently measured parameter accessible from neutron scattering or from spontaneous mechanical distortions on going from the nematic to isotropic phase. Unless there is a large nematic order change induced by $\underline{\underline{\lambda}}$, the shape $\underline{\underline{\ell}}$ is essentially just a rotated version of $\underline{\underline{\ell}}_0$, a uniaxial ellipsoid with the long axis (at $r>1$) oriented along $\mathbf{n}$ instead of $\mathbf{n}_0$.

Embedded in the general expression (2) is the penalty for local director deviations from the orientation $\mathbf{n}_0$ imprinted into the network at formation. When no elastic strains are allowed, $\underline{\underline{\lambda}} = \underline{\underline{\delta}}$, this elastic energy reduces to

$$F = \frac{3}{2}\mu + \frac{1}{2}\mu\frac{(r-1)^2}{r}\sin^2\Theta, \tag{4}$$

where Θ is the local angle between $\mathbf{n}$ and $\mathbf{n}_0$. The $\sin^2\Theta$ term describes the anchoring towards the original director orientation. The elastic penalty for deviating from its original orientation, appropriately proportional to the square of chain anisotropy, gives the coefficient D_1 of the de Gennes' phenomenological expression at small deformations, Eq. (1). This has to be compared with the Frank elastic penalty for director curvature deformations, $\frac{1}{2}K(\nabla\mathbf{n})^2$. The length scale $\xi \sim (1/r-1)\sqrt{K/\mu}$ at which the two energy contributions are comparable is usually small: $\xi \sim 10^{-8}$ m for a typical $K \sim 10^{-11}$ J/m, $\mu \sim 10^5$ J/m^3 and not too small anisotropy r. This is rather less than the cholesteric pitch p, which is a characteristic scale in our problem. Therefore the anchoring of the director $\mathbf{n}$ to the rubbery matrix, described by Eq. (2), tends to dominate over Frank elasticity effects.

We shall assume that a cholesteric elastomer is locally like a nematic in its elastic response: rubber elasticity is determined on the scale of network crosslink separations (a few nanometers), whereas cholesteric pitches are 10^3 times longer. We can at once see why the chiral structure is stable but how mechanical fields can destabilize it. With no elastic strain, the free-energy penalty is $\sim \frac{1}{2}D_1(\phi-\phi_0)^2$ for rotating the director away from its original helical texture $\phi_0 = q_0 z$. On the other hand, if strains are applied, the rubber can lower its elastic energy (2) by rotating the director $\mathbf{n}$ towards the axis of principal extension. This general principle of adjusting the microstructure to minimize the elastic energy is seen in its ultimate form in the effect of soft elasticity [17,18], when a stretched nematic rubber may reduce its effective modulus (the slope of a stress-strain curve) to zero by optimizing the director rotation and associated shear strains.

Distortions in a cholesteric elastomer cannot be soft, because of elastic compatibility constraints (see Sec. A of the Appendix for more details) in matching different director and shear modes along the helix. Essentially, the soft modes depend on the director orientation, ϕ_0, which vary according to position. This variation gives rise to a shear λ_{yz} that diverges as the linear y dimension of the sample. We accordingly take transverse contractions to be *uniform*. Such deformations, e.g., λ_{xx} and λ_{yy} for stretching along the helix axis z, have to be equal by symmetry and therefore $\lambda_{xx} = \lambda_{yy} = 1/\sqrt{\lambda}$, the classical forms. In contrast, for stretching perpendicular to the helix, the transverse contractions λ_{zz} and λ_{yy} should not be symmetric since one of them is along and the other perpendicular to the coarse-grained principal axis of the helix, z. Indeed, we shall find nonclassical exponents of 2/7 and 5/7 for these relaxations. The incompressibility constraint maintains the relation $\lambda_{zz}\lambda_{yy} = 1/\lambda$.

III. TRANSVERSE ELONGATION

We first consider an imposed stretch in the transverse direction perpendicular to the pitch axis, $\lambda_{xx} = \lambda$. The strain tensor is then in the following form:

$$\underline{\underline{\lambda}} = \begin{pmatrix} \lambda & 0 & 0 \\ 0 & \lambda_{yy} & 0 \\ 0 & 0 & \lambda_{zz} \end{pmatrix}. \tag{5}$$

Although one expects the director rotation in the azimuthal plane x-y (cf. Fig. 1), there are no associated shear strains.

Such shears, $\lambda_{xy}(z)$ and $\lambda_{yx}(z)$, would both lead to elastic compatibility problems, see the Appendix, and we assume they are suppressed. The shears $\lambda_{xz}(z)$ and $\lambda_{xz}(z)$ are not subject to compatibility requirements. However, they should not appear on symmetry grounds, which is easily confirmed by direct minimization. Now $\mathbf{n}_0=\{\cos\phi_0,\sin\phi_0,0\}$ and the rotated director after deformation is $\mathbf{n}=\{\cos\phi,\sin\phi,0\}$. Note that the helix is $\phi_0=q_0z$ in the initial undistorted material. After deformation, because of the uniform affine contraction λ_{zz}, the material frame shrinks and the effective helical pitch becomes $\tilde{q}=q_0/\lambda_{zz}$ in all expressions below. The $\underline{\underline{\ell}}_0$ and $\underline{\underline{\ell}}$ implied by these $\mathbf{n}_0$ and $\mathbf{n}$ via equation (3), take the forms

$$\underline{\underline{\ell}}_0=\begin{pmatrix} l_\perp s_0^2+l_\parallel c_0^2 & (l_\parallel-l_\perp)\ s_0c_0 & 0 \\ (l_\parallel-l_\perp)s_0c_0 & l_\parallel s_0^2+l_\perp c_0^2 & 0 \\ 0 & 0 & l_\perp \end{pmatrix} \tag{6}$$

and

$$\underline{\underline{\ell}}^{-1}=\begin{pmatrix} l_\perp^{-1}s^2+l_\parallel^{-1}c^2 & (l_\parallel^{-1}-l_\perp^{-1})sc & 0 \\ (l_\parallel^{-1}-l_\perp^{-1})sc & l_\parallel^{-1}s^2+l_\perp^{-1}c^2 & 0 \\ 0 & 0 & l_\perp^{-1} \end{pmatrix}, \tag{7}$$

where c_0 and s_0 are shorthand for $\cos\phi_0$ and $\sin\phi_0$; analogously, c and s stand for $\cos\phi$ and $\sin\phi$. Substitution of the above three equations into the free-energy density (2) then yields

$$F_\perp=\frac{1}{2}\mu\Big(\lambda^2+\lambda_{yy}^2+\lambda_{zz}^2+\frac{r-1}{r}[\lambda^2(r\,c_0^2s^2-c^2s_0^2) +\lambda_{yy}^2(r\,c^2s_0^2-s^2c_0^2)-2\lambda\,\lambda_{yy}(r-1)s_0c_0sc]\Big). \tag{8}$$

The appearance of terms linear and quadratic in ϕ (or rather in $\sin\phi$ because all values of the azimuthal angle will be found along the cholesteric helix) indicate that rotations can always lower the energy for $\lambda\neq1$. Incompressibility requires $\lambda_{yy}\lambda_{zz}=1/\lambda$. Minimization of $F_\perp$ with respect to the current director orientation ϕ results in the expression for the local director angle $\phi(z)$ at a given imposed extension λ depending on the initial phase of cholesteric helix ϕ_0,

$$\tan2\phi=\frac{2\lambda\lambda_{yy}(r-1)\sin2\phi_0}{(r-1)(\lambda^2+\lambda_{yy}^2)\cos2\phi_0+(r+1)(\lambda^2-\lambda_{yy}^2)}. \tag{9}$$

Substituting this director profile into $F_\perp$ gives the free-energy density after director rotation. The total free energy then needs to be optimized with respect to the transverse contraction λ_{yy}. This leads to

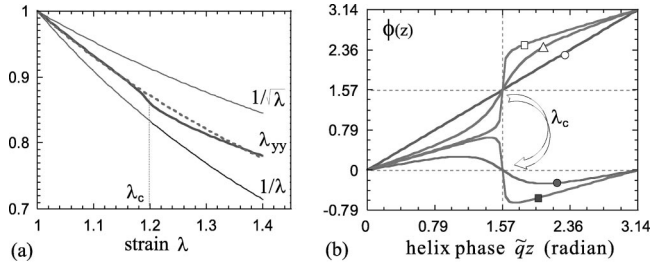

FIG. 2. (a) The transverse contraction λ_{yy} as a function of imposed $\lambda_{xx}=\lambda$. Solid line shows the exact numerical solution of the coarse-graining problem for $r=1.9$; one can see the kink where the discontinuous transition at $\lambda_c=r^{2/7}\approx1.2$ takes place. The dashed line is an interpolation by $\lambda_{yy}=\lambda^{-3/4}$, two thin lines show classical regimes of $\lambda_{yy}=1/\sqrt{\lambda}$ and $1/\lambda$. (b) The director angle ϕ against the cholesteric helix phase q_0z for increasing strain $\lambda=1$ (open circle), 1.15 (triangle), 1.23 (open square), 1.25 (shaded square), and 1.5 (shaded circle). At $\lambda\geqslant\lambda_c$ the director pinning at $\phi=\pi/2$ breaks down and a discontinuous transition occurs, after which the director continuously rotates towards the final uniform $\phi=0$.

$$\frac{\pi}{4}\frac{(r+1)^2}{r}-\frac{\pi}{\lambda_{yy}^4\lambda^2}+\frac{r-1}{r}\int_0^{\pi/2}d\phi_o g=0, \tag{10}$$

where details of the derivation and the definition of g have been relegated to Sec. C of the Appendix. Equation (10) can now be solved numerically, and the solution of optimal λ_{yy} is plotted in Fig. 2(a). This variation is contrasted with two classical regimes—an isotropic 3D contraction $\sim1/\sqrt{\lambda}$ and its 2D equivalent $\sim1/\lambda$ (corresponding to a frozen $\lambda_{zz}=1$). From the plot it is apparent that a good fit is achieved by a power law $\lambda_{yy}\simeq\lambda^{-3/4}$ (and, as a consequence, $\lambda_{zz}\simeq\lambda^{-1/4}$), for the imposed strain λ below the critical value $\lambda_c\simeq r^{2/7}$, when a discontinuous jump in the distribution of director angles occurs, see Fig. 2(b) and also the kink in $\lambda_{yy}(\lambda)$, Fig. 2(a). The critical value $\lambda_c\simeq r^{2/7}$ can be estimated by setting the denominator in equation (9) to zero and taking $\lambda_{yy}\simeq\lambda^{-3/4}$. In fact, a small strain expansion (in $\lambda-1\ll1$) can be made, and it can be shown analytically [19] that the relaxation initially varies as $\lambda_{yy}\simeq\lambda^{-5/7}$ and $\lambda_{zz}\simeq\lambda^{-2/7}$.

Initially, all directors at $0<\tilde{q}z<\pi/2$ (first helical half-turn) are induced to rotate ''backward'' towards $\phi=0$, and all directors at $-\pi/2<\tilde{q}z<0$ (second helical half-turn) rotate ''forward'' towards $\phi=\pi$, as the imposed deformation λ increases, see Fig. 2(b). Although $\phi=0$ and π describe equivalent directors, the twist wall separating these two states becomes sharper and sharper. Due to the helix imprinting, the orientations $\phi=0$ at $\tilde{q}z=0$ and $\phi=\pi$ at $\tilde{q}z=\pi$ are pinned, as is the middle point of the twist wall at $\tilde{q}z=\pi/2$. As a result, no change of the helical pitch apart from the affine contraction $\tilde{q}=q_0/\lambda_{zz}$ can occur. This is in contrast with cholesteric liquid crystals, where in a classical problem of helix unwinding by electric or magnetic field one finds an increase in cholesteric pitch [14,15] along with coarsening of the helix.

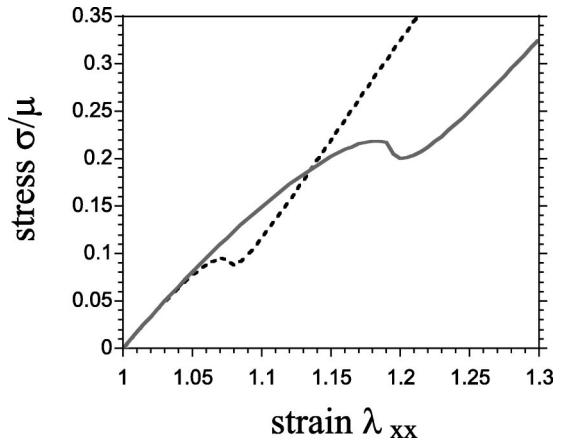

FIG. 3. The nominal stress vs strain relation for a transverse elongation, $r=1.3$ (dashed line) and $r=1.9$ (solid line).

Examining Eq. (9), one finds that as the increasing applied strain reaches a critical value λ_c, the width of the twist wall, centered at $\tilde{q}z=\pi/2$ between the values $\phi=\pi/4$ and $3\pi/4$, decreases to zero and the discontinuous transition occurs. The director in the midpoint of the wall breaks away from the pinning and jumps from $\phi=\pi/2$ to $\phi=0$, along the strain axis, thus removing the topologically constrained twist wall. From this point there is no barrier for director rotation towards the final uniform orientation with $\phi=0$, as the last two curves in Fig. 2(b) indicate. The role of Frank elasticity is discussed at the end.

A discontinuous director jump at a critical strain has been predicted, and indeed observed in nematic elastomers stretched at exactly 90° to their initial director $\mathbf{n}_0$ [17,20]. In a stretched cholesteric, one always finds an exact phase angle $\phi=\pi/2$ along the helix—where the center of narrowing twist wall becomes pinned from both sides. It is this point that experiences a discontinuous jump. Thus λ_c is an upper bound on the stability and the transition. The point of equality of the free energies of the system with and without twist walls occur at a slightly lower $\lambda<\lambda_c$.

The corresponding stress-strain $\sigma_{xx}(\lambda)$ relations can be obtained by differentiating the energy, Eq. (8), with respect to λ, and the results are plotted in Fig. 3. We can see that the stress exhibits a dip corresponding to the kink in the transverse relaxation. If a controlled-stress device is used, the material will undergo a sudden jump in length at $\lambda=\lambda_c$. This mechanical instability would be accompanied by the discontinuous jump in the nematic director orientations, which could be monitored optically.

There exists of course intrinsically chiral-elastic coupling, such as terms of the type $A\mathbf{n}\cdot\underline{\underline{\varepsilon}}^{(s)}\cdot[\nabla\times\mathbf{n}]$, introduced by Terentjev [21], Eq. (5). These involve *derivatives* of the nematic director and are therefore smaller by at least a factor of $q_0 a\sim 10^{-4}$, where a is a molecular length of the order of Å.

IV. STRETCHING ALONG THE PITCH AXIS

Having considered the material response under a stretch perpendicular to the helical axis, we now turn our attention to the case of (cf. Fig. 1) an imposed stretch along the helical pitch axis, $\lambda_{zz}=\lambda$. The deformation tensor takes the form of

$$\underline{\underline{\lambda}}=\begin{pmatrix} 1/\sqrt{\lambda} & 0 & \lambda_{xz} \\ 0 & 1/\sqrt{\lambda} & \lambda_{yz} \\ 0 & 0 & \lambda \end{pmatrix}. \tag{11}$$

No compatibility problem with shears $\lambda_{xz}(z)$ and $\lambda_{yz}(z)$ arises from their variation with z along the helical pitch. By contrast, their conjugate strains λ_{zx} and λ_{zy}, which would also have to vary with z, lead to a serious compatibility mismatch, e.g., $\partial\lambda_{zx}/\partial z=\partial\lambda_{zz}/\partial x$. We therefore deduce that λ_{zx} and λ_{zy} are suppressed even though in other settings [17] these are the generators of soft elastic response. Conceivably, λ_{xy} and λ_{yx} could exist, but that seems unlikely as numerical tests would suggest (see Section B of the Appendix).

In this geometry one expects the director to rotate by θ out of the azimuthal x-y plane, see Fig. 4(a). The initial director orientation is, as before, $\mathbf{n}_0=\{\cos q_0 z,\sin q_0 z,0\}$, while after deformation the rotated director is aligned along the surface of a cone: $\mathbf{n}=\{\cos\theta\cos\tilde{q}z,\cos\theta\sin\tilde{q}z,\sin\theta\}$. As in the case of a transverse stretch (previous section), all physical dimensions in the deformed sample are scaled by the affine strain. In particular, here $z\to\lambda z$, resulting in the corresponding expansion of the cholesteric pitch, $\tilde{q}=q_0/\lambda$. With the $\underline{\underline{\ell}}_0$ and $\underline{\underline{\ell}}$ defined by the axes $\mathbf{n}_0$ and $\mathbf{n}$, the free-energy density (2) now becomes a function of three variables: the director tilt angle θ and the two shear strains $\lambda_{xz}(z)$ and $\lambda_{yz}(z)$ (we continue to neglect the effects of director gradients and Frank elasticity). Algebraic minimization over these components of strain tensor is not difficult. Without loss of generality, we take $q_0 z=\tilde{q}z=0$ (all other values of $q_0 z$ are related by rotational symmetry), then we have

$$\underline{\underline{\ell}}_0=\begin{pmatrix} \ell_\parallel & 0 & 0 \\ 0 & \ell_\perp & 0 \\ 0 & 0 & \ell_\perp \end{pmatrix} \tag{12}$$

and

$$\underline{\underline{\ell}}^{-1}=\begin{pmatrix} \ell_\perp^{-1}\sin^2\theta+\ell_\parallel^{-1}\cos^2\theta & 0 & (\ell_\parallel^{-1}-\ell_\perp^{-1})\sin\theta\cos\theta \\ 0 & \ell_\perp^{-1} & 0 \\ (\ell_\parallel^{-1}-\ell_\perp^{-1})\sin\theta\cos\theta & 0 & \ell_\parallel^{-1}\sin^2\theta+\ell_\perp^{-1}\cos^2\theta \end{pmatrix}, \tag{13}$$

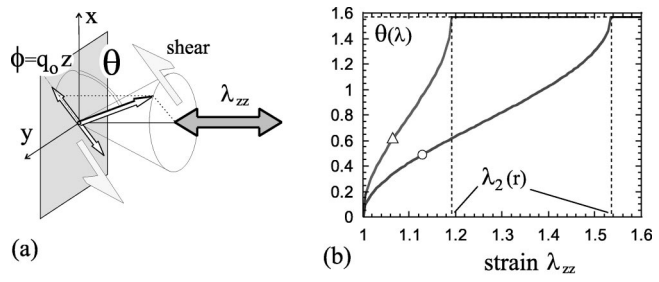

FIG. 4. (a) The geometry of director rotation in response to stretching λ_{zz} along the helix axis. (b) The angle θ of director tilt plotted against the imposed strain λ, Eq. (18), for $r=1.3$ (triangle) and $r=1.9$ (circle). Strain varies from 1 to $\lambda_2=r^{2/3}$ at which point the alignment is $\theta=\pi/2$, uniformly along the former pitch axis.

giving rise to a free-energy density

$$F_{\parallel}=\frac{1}{2}\mu\left[\frac{r\sin^2\theta+\cos^2\theta+1}{\lambda}+\lambda^2\left(\frac{1}{r}\sin^2\theta+\cos^2\theta\right)+\lambda_{yz}^2 + 2\lambda_{xz}\lambda\left(\frac{1}{r}-1\right)\sin\theta\cos\theta+\lambda_{xz}^2\left(\sin^2\theta+\frac{1}{r}\cos^2\theta\right)\right]. \tag{14}$$

Optimizing for the shears λ_{xz} and λ_{yz} gives

$$\lambda_{xz}=\lambda\frac{(r-1)\sin 2\theta}{(r+1)-(r-1)\cos 2\theta},\quad \lambda_{yz}=0.$$

This represents a strain made up of displacements in the direction of **n** projected into the x-y plane and varying with z. Generalizing to the $q_0 z\neq 0$ case, we have

$$\begin{pmatrix}\lambda_{xz}\\ \lambda_{yz}\end{pmatrix}=\frac{\lambda}{2}\frac{(r-1)\sin 2\theta}{r+1-(r-1)\cos 2\theta}\begin{pmatrix}\cos\tilde{q}z\\ \sin\tilde{q}z\end{pmatrix}, \tag{15}$$

in phase with the azimuthal angle along the helical pitch. Equation (15) describes the z variation of distortions within the x-y plane in the direction of the initial director $\mathbf{n}_0$ and perpendicular to the helix axis. On substitution of these optimal shears back into the free-energy density one obtains

$$F_{\parallel}=\frac{1}{2}\mu\left(\frac{\lambda^2}{1+(r-1)\sin^2\theta}+\frac{2+(r-1)\sin^2\theta}{\lambda}\right). \tag{16}$$

$F_{\parallel}$ expands at small tilt angle θ as

$$F_{\parallel}\approx\tfrac{1}{2}\mu(\lambda^2+2/\lambda)-\tfrac{1}{2}\mu\,\theta^2(r-1)(\lambda^2-1/\lambda), \tag{17}$$

that is, the director starts to rotate down to define a cone of semiangle $\pi/2-\theta$ immediately as the strain $\lambda>1$ is imposed. The equilibrium director tilt is obtained by minimization of the full free-energy density $F_{\parallel}(\theta)$,

$$\sin^2\theta=\frac{\lambda^{3/2}-1}{r-1},\quad \theta=\arcsin\sqrt{\frac{\lambda^{3/2}-1}{r-1}}. \tag{18}$$

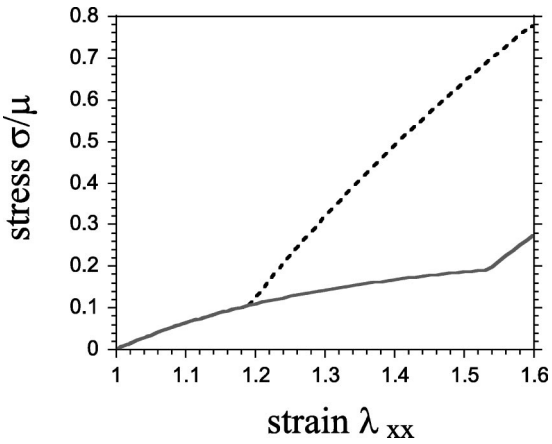

FIG. 5. The nominal stress vs strain relation for a stretch along the pitch axis, $r=1.3$ (dashed line) and $r=1.9$ (solid line).

The director rotation starts and ends in a characteristically singular fashion, Fig. 4(b) (reminiscent of the universal optomechanical response seen in soft nematic elastomers [22]). The rotation is complete, with the director aligned along the extension axis ($\theta=\pi/2$) at $\lambda=r^{2/3}$, which for some elastomers, can be a very large extension.

The corresponding stress-strain plots are shown in Fig. 5. The material hardens significantly after reaching λ_2, which reflects the fact that the material no longer has the freedom to rotate its director in its attempt to lower free energy.

V. EFFECT OF AN AXIAL ELECTRIC FIELD

It has been reported that an electric field applied along the pitch axis can have a similar effect of reorienting the director towards the pitch axis; a history-dependent critical field is required and this effect can be utilized to make data storage media [9]. Moreover, the recovered ($E=0$) state is monodomain, in contrast to those commonly found for liquid cholesterics. This is also an easily accessible experimental geometry, since the initial director is in the plane of a flat sample film, with the helical axis and the applied field along the sample normal. An electric voltage V, applied across the sample of thickness $d=\lambda d_0$, adds an extra term to the free-energy equation (16),

$$F_E=-\frac{1}{2}\Delta\epsilon\epsilon_0\frac{V^2}{\lambda^2 d_0^2}\sin^2\theta, \tag{19}$$

where $\Delta\epsilon$ is the differential dielectric constant. So we have

$$F_{\parallel,E}=\frac{1}{2}\mu\left(\frac{\lambda^2}{1+(r-1)\sin^2\theta}+\frac{2+(r-1)\sin^2\theta}{\lambda}\right) -\frac{1}{2}\Delta\epsilon\epsilon_0\frac{V^2}{\lambda^2 d_0^2}\sin^2\theta. \tag{20}$$

It is clear that the electric field alters the coefficient of the $\sin^2\theta$ term, and the tilt angle after minimizing the free energy is now

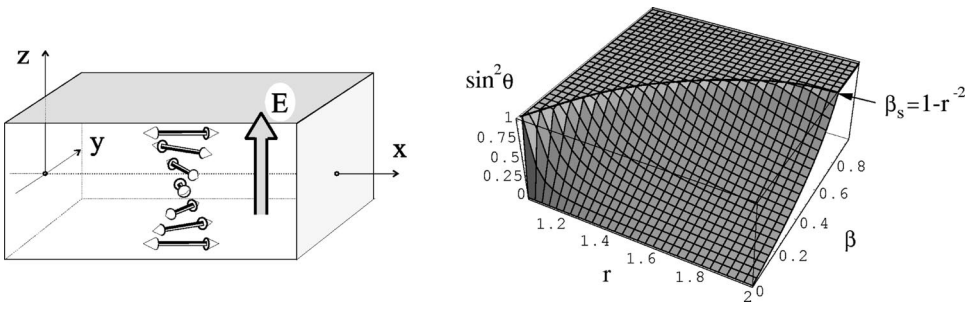

FIG. 6. A cholesteric elastomer in an electric optic device geometry. Director orientation $\sin^2\theta$ is shown as a function of anisotropy r and reduced electric field β. The reduced electric field required to complete θ rotation to $\pi/2$ is given by $\beta_s = 1 - r^{-2}$.

$$\sin^2\theta = \frac{\sqrt{\lambda^4/(\lambda-\beta)}-1}{r-1}, \tag{21}$$

with $\beta = (\Delta\epsilon\epsilon_0 V^2)/(r-1)\mu d_0^2$ and λ is to be determined by boundary and minimization conditions. If no field is applied, $\beta = 0$, we retrieve equation (18) of the previous section. The dimensionless β measures the effect of an applied electric field in units of the nematic anisotropy energy, $(r-1)\mu$.

We discuss the two following cases: a clamped elastomer where $\lambda = \lambda_{zz} = 1$ is enforced, and a free-standing elastomer where electrodes are painted on and λ can relax.

(i) In the clamped case, there is no deformation, $\lambda = 1$, we have

$$\sin^2\theta = \frac{(1-\beta)^{-1/2}-1}{r-1}. \tag{22}$$

Hence there is a continuous rotation of the director orientation towards the pitch axis as we slowly increase the electric voltage until saturation,

$$V_s = d_0\sqrt{\frac{\mu(r^2-1)(r-1)}{\Delta\epsilon\epsilon_0 r^2}} \quad \text{or} \quad \beta_s = 1 - r^{-2}, \tag{23}$$

at the point at which θ reaches $\pi/2$ and remains so, see Fig. 6, thereafter for $V > V_s$. (ii) When λ can relax to further lower the energy, we must return $\sin^2\theta$ from Eq. (21) to the energy expression (20),

$$F_{\parallel,E} = \frac{1}{2}\mu\left(2\sqrt{\lambda-\beta} + \frac{1}{\lambda} + \frac{\beta}{\lambda^2}\right), \tag{24}$$

before minimizing over λ. The minimization cannot be carried out analytically in general, but in the limit of small $\beta \ll 1$ it leads to $\sin^2\theta_E = (2\beta/r-1) + O(\beta^2)$ with

$$\lambda_E = 1 + \beta - 2\beta^2 + O(\beta^3) \quad \text{and}$$

$$F_E = \tfrac{1}{2}\mu[3 - 2\beta^2 + O(\beta^3)].$$

In both cases, clamped or free, shears $\lambda_{n_0 z}$ are induced, see Eq. (15), which involve displacements perpendicular to the electric field. Any residual dust particles will be displaced and become tracers of mechanical deformations as in electrical experiments on nematic gels n Fredericks geometry [25].

We do not predict rotational effects of the director about the helix axis as suggested by Brand [23] (who was not concerned with the rotatory-mechanical effects of our earlier section) for reasons that have been explored by Refs. [21,24].

VI. DISCUSSION

In contrast to conventional cholesteric liquid crystals, we have altogether ignored effects of Frank elastic energy. The most compelling evidence for this is the very stability of the imprinted helical state in the face of the Frank penalty $\frac{1}{2}K_2 q_0^2$. The argument for this relies upon the great difference in characteristic length scales, the elastomer penetration depth, more accurately expressed as ξ [cf. Eq. (4)], and the director modulation wavelength estimated by the helical pitch $p = \pi/q_0 \gg \xi$. There are two possibilities to alter this inequality—by increasing the penetration depth ξ (either by making a weaker gel, or a less anisotropic one), or by locally increasing the director gradient (e.g., in the evernarrowing twist wall, Fig. 2). As the width of the twist wall decreases to zero, the Frank energy density grows and diverges at the critical strain λ_c. Therefore the local analysis of Eqs. (8) and (9) is only valid outside the region of strain $\Delta\lambda \sim (q_0\xi)^2$ around λ_c. In a typical hard nematic rubber this is a very small deviation, not altering the conclusions drawn, but in a weak gel with low chain anisotropy it may become more substantial. Also, the actual finite width of the twist wall at the transition, may raise the question of topological mechanism for eliminating the twist stored in the cholesteric helix, perhaps by a disclination loop expansion in the x-y plane. The dynamics of such disclination loop would require further studies.

One can estimate how weak a gel must be for the Frank elasticity to intervene in our analysis in a more substantial way. When $\xi \sim p$, for example, with a pitch $p \sim 4 \times 10^{-7}$ m, then a rubber modulus of only $\mu \sim 60$ J/m^3 is required (assuming $[r-1] \sim 1$). Nematic elastomers typically have $\mu \sim 10^3 - 10^5$ J/m^3 and their cholesteric analog would clearly find Frank-elastic effects minor. However, an elastomer with a reasonable $\mu \sim 10^3$ J/m^3 would feel the director gradients when its polymer chain anisotropy becomes as low as $r = \ell_\parallel/\ell_\perp \sim 1.25$. Such a low value is often found in sidechain liquid crystal polymers, especially near the clearing point [17]. The situation where Frank elasticity becomes significant is complex. Qualitatively, in penalizing the director gradient, the Frank elastic term will increase the critical λ_c in the case of transverse elongation and facilitate the conical formation for the case of stretching along the pitch axis.

To summarize, we have analyzed a qualitatively new response of an elastomer with chiral cholesteric microstructure to applied fields that is different from classical cholesteric liquids. Likewise, the chiral imprinting and its modification by elastic fields is a new effect in rubbers and solids. Furthermore, we have shown that one could modify these effects by the use of electric field that can give rise to new electro-optical devices. Other possibilities include solvents (with or without chiral power) and magnetic fields.

ACKNOWLEDGMENTS

We would like to thank T. C. Lubensky and R. B. Meyer for useful discussions.

APPENDIX

1. Mechanical compatibility

Generally, material deformations are finite and continuous lest we break the material. Therefore we require that the displacement vector $\underline{u}(\underline{r})$ should be a continuous function of position $\underline{r}$, and it follows that $\partial_i\partial_j u_k = \partial_j\partial_i u_k$, where $\partial_{i,j,k}$ represent partial differentiations with respect to x,y or z. Since $\lambda_{kj} = \partial_j u_k$, the equivalent constraint on the possible $\underline{\underline{\lambda}}$ is

$$\partial_i \lambda_{kj} = \partial_j \lambda_{ki}; \tag{A1}$$

we refer to these implicit constraints as compatibility requirements. A simple case of incompatibility would be a z-dependent rotation $\alpha(z)$,

$$\underline{\underline{\lambda}}_1 = \begin{pmatrix} \lambda & -\alpha(z) & \lambda_{xz} \\ \alpha(z) & \lambda_{yy} & \lambda_{yz} \\ \lambda_{zx} & \lambda_{zy} & \lambda_{zz} \end{pmatrix}. \tag{A2}$$

To see the incompatibility, we consider the constraint on λ_{xz},

$$\frac{\partial \lambda_{xz}}{\partial y} = -\frac{\partial \alpha(z)}{\partial z}. \tag{A3}$$

At a fixed position z, the right-hand side is a constant independent of y. Hence the integration would lead to divergent values of strain λ_{xz} for $y \to \infty$. Therefore the proposed deformation mode cannot occur. Physically, it corresponds to the case of a small rotation creating a large displacement far away from the rotation axis.

The argument can likewise be made with the soft modes. If the material at a position z attempts a soft deformation, its director rotates towards the x axis. It is known that the elongation λ_{xx}, contraction λ_{yy}, and shear λ_{xy}, are precisely determined by the initial orientation ϕ_0, and the rotation from it, if the process is to be soft. The next slab of material, at $z+dz$, has the initial orientation $\phi_0 + q_0 dz$ and a different set of soft strains $\underline{\underline{\lambda}}$ must arise. Material points at y translate to $\lambda_{yy}(z)\cdot y$ and $\lambda_{yy}(z+dz)\cdot y$ in the two neighboring slabs along the helix, that is they differ by a relative displacement $(\partial\lambda_{yy}/\partial z)dz\cdot y$. There is thus a generated shear $\lambda_{yz} = (\partial\lambda_{yy}/\partial z)\cdot y$ that diverges as the linear y dimension of the sample. We accordingly assert that the transverse contractions are *uniform*. Such deformations, e.g., λ_{xx} and λ_{yy} for stretching along the helix axis z, have to be equal by symmetry and therefore $\lambda_{xx} = \lambda_{yy} = 1/\sqrt{\lambda}$. In contrast, for stretching perpendicular to the helix, the transverse contractions λ_{zz} and λ_{yy} should not be symmetric since one of them is along, and the other perpendicular to, the coarse-grained principal axis of a helix z.

2. Mechanical stability

It is unclear, *a priori*, whether the stretched elastomer would spontaneously undergo complex twists, reaching an inhomogeneous state such as the blue phase [26]. Experimentally [27], samples have been stretched perpendicular to the helix axis, and no complex phase formation has been observed. Below we test for two most obvious modes of mechanical modulations in response to an elongation λ imposed along x axis. The first,

$$\underline{\underline{\lambda}}_1 = \begin{pmatrix} \lambda & \alpha_1 q_y \cos q_y y \cos \tilde{q} z & -\alpha_1 \tilde{q} \sin q_y y \sin \tilde{q} z \\ 0 & \lambda_{yy} & 0 \\ 0 & 0 & \lambda_{zz} \end{pmatrix}, \tag{A4}$$

which corresponds to a displacement vector of $\underline{u} = (\lambda x + \alpha_1 \cos qz \sin q_y y, \lambda_{yy} y, \lambda_{zz} z)$ with the modified pitch $\tilde{q} = q_0/\lambda_{zz}$; note that $\lambda_{ij} = \partial_j u_i$. The second,

$$\underline{\underline{\lambda}}_2 = \begin{pmatrix} \lambda & 0 & 0 \\ 0 & \lambda_{yy} & -\alpha_2 \tilde{q} \sin \tilde{q} z \\ 0 & 0 & \lambda_{zz} \end{pmatrix}, \tag{A5}$$

corresponds to a displacement vector of $\underline{u} = (\lambda x, \lambda_{yy} y + \alpha_2 \cos \tilde{q} z, \lambda_{zz} z)$. The first mode $\underline{\underline{\lambda}}_1$ represents a modulated wave in the plane perpendicular to the pitch axis, and the second mode corresponds to a simple modulation along the pitch axis. To test their stability, we substitute the above $\underline{\underline{\lambda}}$'s into the free-energy density, Eq. (2), and numerically minimize it with respect to the current director orientation, subject to the constant volume constraint $\det(\underline{\underline{\lambda}}) = 1$. Numerical analysis shows that the minimized free energy is quadratic in $\alpha_{1,2}$ with *positive* coefficients. Any other form of mechanical perturbation can be tested for stability in this way, and so far no instability has been found.

3. Derivation of Eq. (10)

Substituting the oscillating expression of $\tan 2\phi$ back into $F_\perp$ and coarse graining it over the helix, we seek the optimal magnitude for the transverse contractions along the pitch λ_{zz}, and in the azimuthal plane λ_{yy}

$$\frac{\partial}{\partial(\lambda_{yy}^2)} \int_0^{\pi/2} d\phi_o F_\perp = 0, \tag{A6}$$

which gives rise to

$$\pi-\frac{\pi}{\lambda_{yy}^4\lambda^2}+\frac{r-1}{r}\int_0^{\pi/2}d\phi_o\left\{[rs_0^2(1+c_2)-c_0^2(1-c_2)]-\frac{\lambda}{\lambda_{yy}}(r-1)s_oc_os_2\right\}=0, \tag{A7}$$

where c_2 and s_2 are shorthand for $\cos 2\phi$ and $\sin 2\phi$. Separating out the c_2 and s_2 terms, the rest can be trivially integrated leading to

$$\frac{\pi}{4}\frac{(r+1)^2}{r}-\frac{\pi}{\lambda_{yy}^4\lambda^2}+\frac{r-1}{r}\int_0^{\pi/2}d\phi_o\left[(rs_0^2+c_0^2)c_2-\frac{\lambda}{\lambda_{yy}}(r-1)s_0c_0s_2\right]=0. \tag{A8}$$

The integrand, after incorporating $\tan 2\phi$ using

$$|c_2|=\frac{1}{\sqrt{1+\tan^2 2\phi}},\quad |s_2|=\frac{\tan 2\phi}{\sqrt{1+\tan^2 2\phi}}$$

with appropriate signs, simplifies to

$$g=-\frac{a_1[1+(r-1)s_0^2]-2r\lambda^2}{\sqrt{a_1^2-4r\lambda^2\lambda_{yy}^2}}, \tag{A9}$$

where

$$a_1=r\lambda^2+\lambda_{yy}^2-(r-1)s_0^2(\lambda^2-\lambda_{yy}^2). \tag{A10}$$

Equation (A8) then becomess

$$\frac{\pi}{4}\frac{(r+1)^2}{r}-\frac{\pi}{\lambda_{yy}^4\lambda^2}+\frac{r-1}{r}\int_0^{\pi/2}d\phi_o g=0. \tag{A11}$$

[1] G. Maxein, S. Mayer, and R. Zentel, Macromolecules **32**, 5747 (1999).
[2] S.T. Kim and H. Finkelmann, Macromolecules **22**, 429 (2001).
[3] P.G. de Gennes, Phys. Lett. **28A**, 11 (1969).
[4] C.D. Hasson, F.J. Davis, and G.R. Mitchell, Chem. Commun. (Cambridge) 2515 (1998).
[5] Y. Mao and M. Warner, Phys. Rev. Lett. **84**, 5335 (2000).
[6] M. Schadt and P. Gerber, Mol. Cryst. Liq. Cryst. **65**, 241 (1981).
[7] D.K. Yang, L.C. Chien, and J.W. Doane, Appl. Phys. Lett. **60**, 3102 (1992).
[8] Y. Mao and M. Warner, Phys. Rev. Lett. **86**, 5309 (2001).
[9] R.A.M. Hikmet and H. Kemperman, Nature (London) **392**, 476 (1998).
[10] V.I. Kopp, B. Fan, H.K.M. Vithana, and A.Z. Genack, Opt. Lett. **23**, 1707 (1998).
[11] H. Finkelmann, S.T. Kim, A. Munoz, B. Taheri, and P. Palffy-Muhoray, Adv. Mater. **13**, 1069 (2001).
[12] M. Warner, E.M. Terentjev, R.B. Meyer, and Y. Mao, Phys. Rev. Lett. **85**, 2320 (2000).
[13] R. Zentel, Liq. Cryst. **3**, 531 (1988).
[14] R.B. Meyer, Appl. Phys. Lett. **12**, 281 (1968).
[15] P.G. de Gennes, Solid State Commun. **6**, 163 (1968).
[16] P.G. de Gennes, in *Liquid Crystals of One- and Two-Dimensional Order*, edited by W. Helfrich and G. Heppke (Springer, Berlin, 1980), p. 231.
[17] M. Warner and E.M. Terentjev, Prog. Polym. Sci. **21**, 853 (1996).
[18] P.D. Olmsted, J. Phys. II **4**, 2215 (1994).
[19] P. Bermel, Masters thesis, Cambridge University, 2001.
[20] G.R. Mitchell, F.J. Davis, and W. Guo, Phys. Rev. Lett. **71**, 2947 (1993).
[21] E.M. Terentjev, Europhys. Lett. **23**, 27 (1993).
[22] H. Finkelmann, I. Kundler, E.M. Terentjev, and M. Warner, J. Phys. II **7**, 1059 (1997).
[23] H.R. Brand, Makromol. Chem., Rapid Commun. **10**, 441 (1989).
[24] R.A. Pelcovits and R.B. Meyer, J. Phys. II **5**, 877 (1995).
[25] E.M. Terentjev, M. Warner, R.B. Meyer, and J. Yamomoto, Phys. Rev. E **60**, 1872 (1999).
[26] P.G. de Gennes and J. Prost, *The Physics of Liquid Crystals* (Oxford University Press, Oxford, 1993).
[27] H. Finkelmann (private communication).